Desalination and Water Treatment
www.deswater.com
doi: 10.1080/19443994.2014.926834

55 (2015) 1453–1466
July

Taylor & Francis
Taylor & Francis Group

Dynamic adsorption of phenolic compounds on activated carbon produced from pulp and paper mill sludge: experimental study and modeling by artificial neural network (ANN)

Mojtaba Masomi[a], Ali Asghar Ghoreyshi[a,*], Ghasem D. Najafpour[a], Abdul Rahman B. Mohamed[b]

[a]*Department of Chemical Engineering, Babol University of Technology, Babol, Iran, Tel. +98 1113234204; Fax: +98 1113234201; emails: mojtabamasomi@yahoo.com (M. Masomi), aa_ghoreyshi@yahoo.com (A.A. Ghoreyshi), Najafpour@nit.ac.ir (G.D. Najafpour)*
[b]*School of Chemical Engineering, Engineering Campus, Universiti Sains Malyasia, Nibong Tebal, Penang, Malaysia, Tel. +60 4 5996410; Fax: +60 4 5941013; email: chrahman@eng.usm.my*

Received 16 November 2013; Accepted 14 May 2014

ABSTRACT

A new low-cost activated carbon (AC) was produced from pulp and paper mill sludge through chemical activation by zinc chloride. Different characterization analyses were carried out on developed AC; these demonstrated a carbon material with highly porous structure. Dynamic adsorption of phenolic compounds (i.e. phenol, 2-chlorophenol, and 4-nitrophenol) from simulated aqueous solution was investigated in a fixed-bed adsorption column using the prepared AC. Dynamic behavior of the adsorption column was assessed in terms of breakthrough curves obtained at different key operating conditions such as bed height, feed flow rate, inlet concentration, and temperature. Sharp breakthrough curves were observed at high-feed flow rate, high-inlet concentration, high temperature, and low-bed height which show the correct dynamic behavior of the adsorption column. The breakthrough times followed the order of 4-nitrophenol > 2-chlorophenol > phenol at all key operating conditions. This arrangement was attributed to their relative adsorption capacities. Data-oriented artificial neural network (ANN) technique along with two empirical physical models (Thomas and Yan model) was employed to characterize breakthrough curves for the adsorption of phenolic compounds through the fixed-bed column. Although, both Thomas and Yan models were able to fit well the breakthrough curves obtained at various operating conditions, a nearly perfect match between experimental breakthrough curves and the predicted ones was attained using ANN. The results of the present study demonstrated that the ANN technique can be employed as a powerful technique for modeling of adsorption process.

Keywords: Phenolic compounds; Dynamic adsorption; Pulp and paper mill sludge; Activated carbon; Modeling; ANN

*Corresponding author.

1. Introduction

Water pollution due to the presence of aromatic materials, especially phenolic compounds in industrial effluents is one of the major environmental problems in the world. Phenol (ph), and its derivatives such as 2-chlorophenol (2-Cph) and 4-nitrophenol (4-Nph) exist in effluents of many industries such as textiles, plastics, steel, herbicides, pesticides, coal tar, synthetic rubbers, pulp mills, pharmaceuticals, petrochemical, and insecticides industries [1,2]. These phenolic compounds are toxic and harmful to organisms and humans even at low concentrations and carcinogenic at high concentrations. In this respect, these compounds are classified as high-priority water pollutants by United States Environmental Protection Agency [3]. Therefore, removal of phenolic compounds from industrial effluents is necessary. There are various technologies for eliminating phenol and its derivatives from aqueous solution such as membrane separation [4], different oxidation processes including catalytic [5], electrochemical and UV [6] and photo oxidation [7], biodegradation [8], photocatalytic conversion [9], and adsorption by different adsorbents [10]. Among the above methods, adsorption by activated carbon (AC) is known as an efficient technique for the removal of many types of pollutants due to easy process design and operation as well as large surface area and high-adsorption capacity provided by ACs [2,11]. However, widespread application of commercial ACs prepared from typical precursors such as various coals and polymers are restricted due to the high cost of these precursors. Therefore, preparation of ACs from low-cost waste materials as precursors could improve the economy of adsorption process. Several researchers have studied the removal of phenolic compounds by AC produced from non-conventional, easily obtainable, and low cost precursors such as palm seed [12], nutshell [13], coconut husk [14], fire wood [15], coffee [16], eucalyptus wood [17], corncob fruit stones [18], and nutshells [19].

Sewage sludge is a carbonaceous material that is produced in municipal and industrial wastewaters treatment plants. The removal of phenolic compounds by low-cost AC produced from sewage sludge was well addressed in the literature [20,21]. The pulp and paper mill sludge (PPMS) is one type of the sewage sludge that is produced from wastewater treatment activities in the pulp and paper industries. It naturally possesses sufficient carbon content because of the wood usage in the paper production process. Therefore, it may be considered as a suitable precursor for production of AC [22,23].

Equilibrium study in a batch adsorption system is useful in identifying effectiveness of the adsorption process and also is necessary to design continuous experiments. However, dynamic adsorption is more applicable in large-scale wastewater treatment plants due to its simplicity as well as easy process scale up. To the best of our knowledge, there is a limited literature about adsorption of phenolic compounds using PPMS-based AC.

The continuous adsorption system in fixed-bed column must be modeled at different experimental conditions (flow rate, influent concentration, bed depth, and temperature) for design and control of adsorption process. Some empirical models such as Thomas [24], Yavuz and Koparal [25], Pandit et al. [26], Agrios et al. [27], and Yan et al. [28] were used for describing the continuous adsorption in fixed-bed column but these models are rather old approximations and are incapable to fit all of continuous adsorption data. Hence, proper modeling of the data obtained in column experiments is one of the principal assignments in adsorption studies.

Data-oriented models such as artificial neural network (ANN) offer a suitable approach for very complex systems with non-linear relationships between variables as well as handling the systems for which relationships are less known. ANN has been greatly used to simulate adsorption processes [29,30]. Some researchers have investigated modeling of phenol adsorption in batch mode by ANN [31]. But a few researchers focused on dynamic adsorption [32,33]. Also, a little attention was paid to the dynamic adsorption of phenol in the fixed-bed AC column [34].

With the background given above, the primary aim of the present research work was to develop a new low-cost AC from PPMS with high-textural characteristics and its application for the removal of phenolic compounds from aqueous solution in a fixed-bed column. The effect of important operational factors such as flow rate, inlet concentration, bed depth, and temperature on the removal of phenolic compounds was investigated. The second task of present study was modeling of column behavior by common physical models such as Thomas and Yan equations as well as mathematical model based on ANN. In this regard, a three-layer ANN model using a back-propagation (BP) algorithm was suggested to predict the breakthrough curve for adsorption of phenolic compounds from aqueous solution by PPMS-based AC. The optimal network structure was attained by an optimization study. Finally, outputs obtained from the optimal ANN modeling were compared to empirical physical models (Thomas and Yan models) and the obtained experimental data.

2. Materials and methods

2.1. Materials

Potassium hexacyanoferrate(III), 4-amino-2,3-dimethyl-1-phenyl-3-pyrazolin-5-one, potassium dihydrogen phosphate, phenol and 2-nitrophenol, hydrochloric acid fuming 37%, NaCl, NaOH, and HCl solution were provided from Merck (Darmstadt, Germany). The 26% ammonia solution and 2-chlorophenol were purchased from Riedel-de Haën, Germany and BDH limited Poole England, respectively. All of the chemicals were of analytical grades and used without any further processing.

2.2. Preparation of AC and its characterization

The PPMS was collected from the treatment plant of the paper making factory (CHOKA, Gilan, Iran). The elemental analysis of the PPMS used as the precursor is summarized in Table 1.

To prepare AC, the PPMS was crushed and sieved to a uniform particle size of 25 mesh after drying at 108°C for 12 h. The dried and powdered PPMS was chemically activated with following method: First, it was soaked within $ZnCl_2$ solution with impregnation weight ratio of 0.9:1 ($ZnCl_2$ to dried PPMS) at 80°C for 6 h. The resulted homogeneous slurry was dried at 108°C for 12 h. Then it was crushed and sieved to a uniform particle size of 25 mesh. The crushed activated solid was then carbonized under constant nitrogen flow rate of 300 ml/min and heating rate of 20°C/min in a vertical tubular furnace at 540°C for 25 min. The activated product was washed with a solution of 5 M HCl to eliminate the remaining $ZnCl_2$ and the portion of soluble ash. Next, it was rinsed with distilled water until the final pH of the washing solution reached to 6–7. Lastly, the synthesized AC was dried at 106°C for 12 h.

Different techniques were used to characterize the prepared PPMS-based AC. Scanning electron microscopy (SEM), N_2 adsorption/desorption isotherms (BET), and Fourier Transform Infrared Spectroscopy (FTIR) analysis were used to determine the surface morphology, textural properties, and functional groups of the AC surfaces, respectively.

2.3. Fixed-bed adsorption experiments

Fixed-bed adsorption study was conducted in a column made of Pyrex glass tube of 6 mm inner diameter and 9 cm total height. Fig. 1 shows the schematic diagram of experimental setup used for dynamic adsorption study. On the top of the column, a ceramic sintered glass was mounted to keep the adsorbent fixed in the column. The column outside was covered by a layer of glass wool for thermal insulation of the column. A definite quantity of the prepared PPMS-based AC was packed in the adsorption column to supply desired carbon bed height of 2, 4, and 6 cm (equivalent to 0.1, 0.2, and 0.3 g of AC). Phenolic compounds solutions with different concentrations (50–400 mg/l) were pumped upward through the column at different feed flow rates (2, 3.5, and 5 ml/min) and different temperatures (20, 35, and 50°C) by a peristaltic pump (Master flux, Cole–Parmer Instrument Co.). The pH of influent solution was set on neutral value (7) in all column experiments. Phenolic compounds solutions at the outlet of the column were collected at definite time interval and the concentrations were estimated by a UV–vis spectrophotometer (model 2100 SERIES, UNICO) at 460, 470, and 500 nm wavelength to determine the concentrations of 2-Cph, ph, and 4-Nph, respectively. In this manner, the breakthrough curves representing dynamic adsorption of phenolic compounds onto the PPMS-based AC fixed-bed column were determined at different key operating conditions.

3. Theoretical study

In this study, two different approaches were adapted to model the dynamic behavior of the adsorption column for the removal of phenolic compounds.

3.1. Physical models

Column experiments are conducted to achieve a breakthrough curve for calculating the maximum adsorption capacity of the adsorbent. Also, the resulted parameters can be utilized in the design, scale up and operation of adsorption column. The exact breakthrough curves for adsorption of an adsorbate in

Table 1
Elemental analysis of PPMS (wt%)

C	N	P	Ca	Si	Mg	Ash	Humidity (infactory)
44.8	0.4	0.054	1.25	30.7	0.17	36.4	70

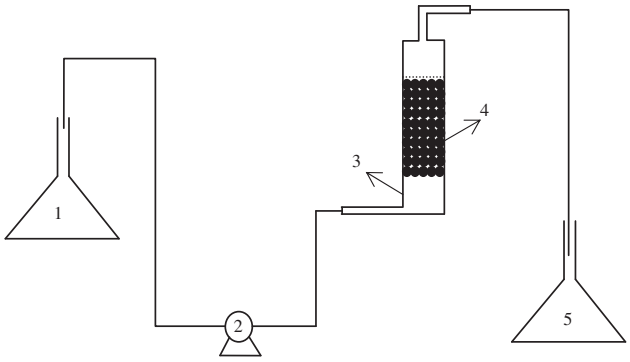

Fig. 1. Schematic diagram of fixed-bed adsorption. 1: Phenolic compounds solution container, 2: peristaltic pump, 3: fixed bed column, 4: adsorbent, 5: adsorbing effluent solution bottle.

column study are obtained by solving complex partial differential equations describing mass transfer for the both bulk fluid and adsorbed phases. However, the simplified empirical equations are frequently used for this purpose [35]. In this study, two well-established models were applied for this purpose. Thomas and Yan models have been widely used in describing dynamic performance of adsorption and are expressed in the following form, respectively:

$$\frac{C}{C_0} = \frac{1}{1 + \exp\left(\frac{K_{Th} q_{Th} m}{Q} - 1000 K_{Th} C_0 t\right)} \tag{1}$$

$$\frac{C}{C_0} = 1 - \frac{1}{1 + \left(\frac{Q}{K_Y q_Y m} t\right)^{\left(\frac{K_Y C_0}{Q}\right)}} \tag{2}$$

where C is the effluent solute concentration (mg/l), C_0 is the solute influent concentration (mg/l), m is the mass of the adsorbent (g), Q is the volumetric flow rate (ml/min), and t is the time (min), q_{Th} and q_Y are the maximum adsorption capacity (mg/g) estimated by Thomas and Yan models, respectively. Also, K_{Th} and K_Y are the kinetic adsorption rate constants for the Thomas and Yan models (ml/mg/min), respectively. A non-linear regression analysis was performed with Matlab software 7.14.0.739 (R2012.a) in order to determine the values of q_T, q_Y, K_{Th}, and K_Y constants. Regression coefficient (R^2) was calculated to evaluate the fitness of models with experimental data.

3.2. Data-oriented ANN model

ANN is a data-oriented mathematical model which is used as an alternative to handle modeling of complex systems for which physical modeling is difficult to be carried out. The key components in ANNs are artificial neurons that conduct basic processing of information. The neurons exist in layers. ANNs have been mainly consisted of three layers: input layer, hidden layer, and output layer. Larger numbers of neurons in the hidden layer give the network more flexibility. However, the too large hidden layer sometimes result in over-fitting and under-characterizing [32].

Experimental data are divided into three subsets: training, testing, and validating set data. Test data are used as a further check that the network is generalizing well, but do not have any effect on training and validation data which are used to stop training early [36].

The most popular ANN is the back-propagation ANN (BP-ANN) [37]. Learning and training are the main computational section in ANNs. The weights of the neurons are modified by learning in neural network according to the error between the values of actual output and output of ANN [29].

The Levenberg–Marquardt (LM) learning algorithm is considered as the most effective algorithm in terms of speed and memory usage. Multilayered feed-forward ANN (ML-ANN) is strong in modeling of non-linear relationship. In this study, we preferred to utilize ML-ANN architecture because of its wide applications in the chemical engineering process. The LM algorithm appears to be the fastest method for training intermediate-sized feed-forward neural networks [31]. ML-ANN is trained in a batch mode using LM BP. The LM algorithm uses the approximation Hessian matrix in the following Newton-like update:

$$w_{k+1} = w_k - [J^T J + \mu I]^{-1} J^T E \tag{3}$$

where w is weight or bias, J is Jacobian matrix, and E is error matrix that is calculated as follow [31]:

$$E = \sum_{j=1}^{k} \sum_{j=1}^{n} (a_i(j) - t_i(j)) \tag{4}$$

where $a_i(j)$ and $t_i(j)$ are the simulated and targeted values, respectively. The term n is the number of output nodes and k is the number of training samples.

The weights and biases are adjusted based on the gradient descent with momentum weight and bias learning function that is indicated as follows:

$$\Delta W_{ij}(k) = \alpha(1 - \beta) \frac{\partial E}{\partial W_{ij}} + \beta \Delta W_{ij}(k - 1) \tag{5}$$

where ΔW_{ij} (n) and ΔW_{ij} ($n-1$) are weights increment between nodes i and j during adjacent iteration. The term α is learning rate and β is momentum constant. Learning rate and momentum constant are chosen 0.01 and 0.9, respectively.

Tangent sigmoid transfer function used for first and second hidden layer and linear transfer function applied for output layer. The input and the target data are processed before training to fall in the range of [–1,1] to provide a better coverage for performance goal [37].

There is no precise available law to make a decision what architecture of ANN and which training and learning algorithm will be better to solve a given problem. In this case, trial and error is the best way. The number of layers, the number of neurons in each layer, the transfer function of neurons in each layer, training, and learning algorithm may be different in various architectures. In this study, no trial and error has been done to obtain optimum transfer functions, learning and training algorithms. They have been selected based on previous well-know experiences [38,39] as was reported in Table 5. However, trial and error was carried out to determine the optimized number of hidden layer as well as number of neurons in each layer within ANN architecture.

4. Results and discussion

4.1. PPMS-based AC characterization

4.1.1. BET surface area

The N_2 adsorption–desorption isotherm of the PPMS-based AC has exhibited the type IV isotherm according to IUPAC classification. The BET (Brunauer–Emmett–Teller) surface area of the synthesized AC was obtained using N_2 adsorption isotherms at 77 K. The main textural properties as well as pH_{PZC} of the prepared PPMS-based AC are given in Table 2.

Table 2
Some textural properties of the prepared PPMS-based AC

Textural properties	Values
Average pore size (nm)	3.13
Total pore volume (cm^3/g)	0.71
Microspore volume (cm^3/g)	0.42
BET surface area (m^2/g)	907.20
pH_{PZC}	4.6

As it can be observed from pH_{PZC} value in Table 2, surface of the prepared AC is charged positively rather than negatively. Also, it possesses large surface area and micro-pore volume that renders physically it as a suitable porous media for adsorption of phenolic compounds.

4.1.2. FTIR spectroscopy investigations

The FTIR analysis was carried out to identify the main functional groups existing on the prepared AC surface. Fig. 2 shows the FTIR spectrum of the PPMS-based AC in which three major peaks are obvious. As shown in Fig. 1, the peak appearing at 3,450 cm^{-1} can be assigned to hydroxyl –OH. The peak observed at 1,639.2 cm^{-1} is attributed to C–N bond in molecules such as quinines. The band at 1,087 cm^{-1} may be responsible for H-bonding of the phenol unit to the

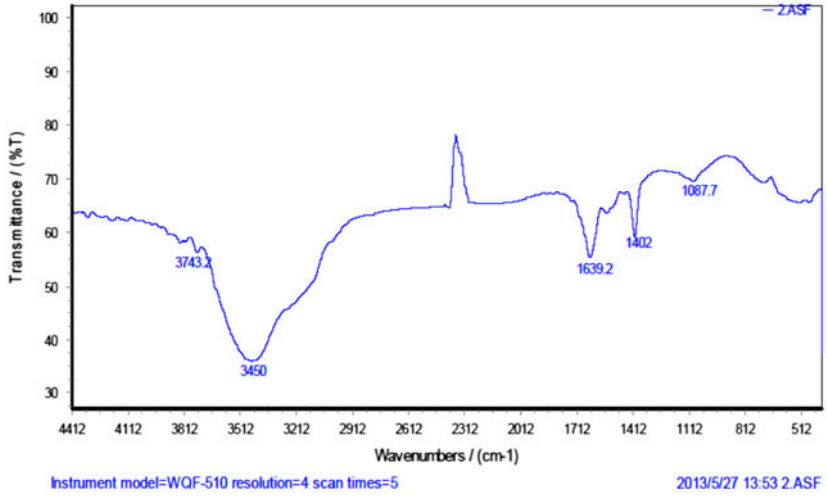

Fig. 2. FTIR spectrum of the synthesized PPMS-based AC.

adsorbent. The hydroxyl groups on the adsorbent surface mainly accounts for the phenols adsorption. Phenolic compounds that can be adsorbed by or react with hydrophobic groups such as –OH group of the adsorbent surface follow the order of 4-Nph > 2-Cph > ph.

4.1.3. SEM–EDX analysis

SEM (VEGA II TESCAN, CZECH) analysis was carried out in order to study surface morphology of PPMS-based AC. The SEM photographs of PPMS-based ACs before and after adsorption of 4-Nph (as an example of adsorbed species) were shown in Fig. 3. It is believed that the porosity of an AC is a function of the used precursor for the synthesis, the method, and the extent of activation. Fig. 2(a) revealed high-porous

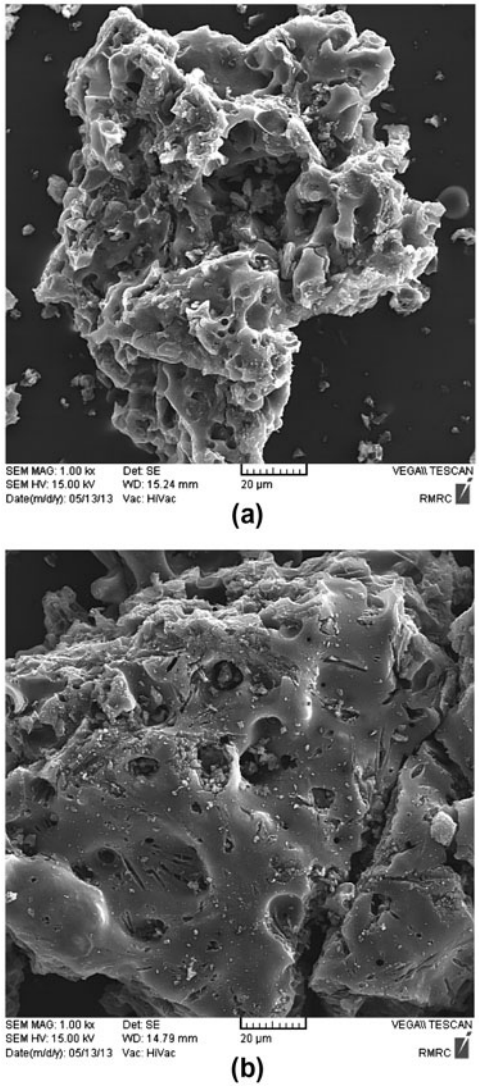

Fig. 3. SEM photographs of the PPMS-based AC: (a) pristine and (b) after adsorption of 4-Nph.

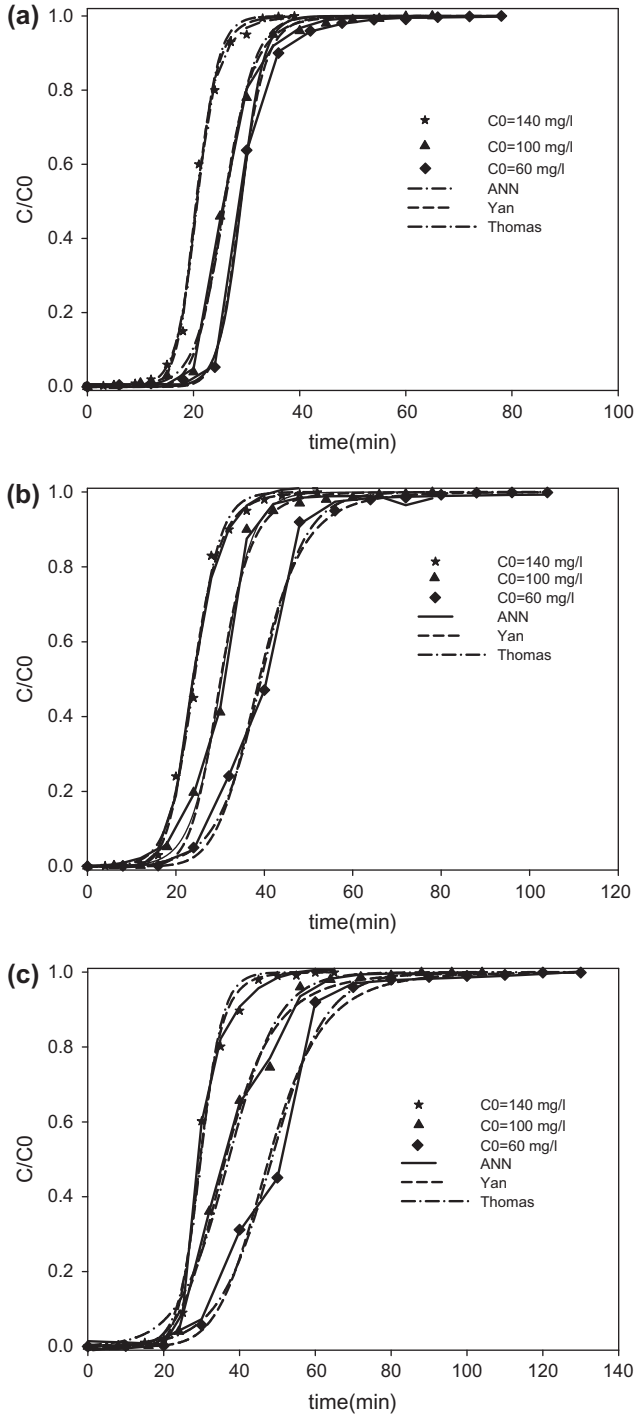

Fig. 4. Breakthrough curves involving experimental data and predicted values by ANN, Thomas and Yan models for adsorption of phenolic compounds onto the PPMS-based AC at different influent concentration [$H = 2$ cm, $Q = 5$ ml/min and $T = 20$°C]. (a) ph, (b) 2-Cph, and (c) 4-Nph.

Table 3
Reference values for input variables and their deviations

Input variable	Bed height (H) cm	Liquid flow rate (Q) ml/min	Inlet concentration (C_i) mg/l	Temperature (T) ℃
Reference value and deviation	4 ± 2	3.5 ± 1.5	100 ± 40	35 ± 15

structure of the pristine PPMS-based AC before the adsorption. From the micrograph, it can be seen that pores are irregular and heterogeneous. Fig. 2(b), represents the micrograph of the adsorbent after adsorption of 4-Nph from its solution with the initial concentration of 200 mg/l. From the image, it is obvious that most of the pores were covered by the adsorbate.

4.2. Effect of operational factors

Dynamic adsorption experiments were performed to determine quantity of the breakthrough curves in the fixed-bed column filled with PPMS-based AC at various key operating conditions. The key operating variables, feed concentration (Fig. 4), bed length (Fig. 5), feed flow rate (Fig. 6), and temperature (Fig. 7) affected strongly on shape of the breakthrough curves. Sensitivity analysis is defined as the ratio of the percentage change of the output to the percentage change of the input with respect to their reference values. Glover and LeVan [40] carried out sensitivity analysis by calculating the derivative of dependent variable with respect to parameters. At the present study to do sensitivity analysis, the differences have been used instead the gradients to determine the relative impact of input variables. Here input variables were bed height, feed flow rate, feed concentration, and temperature. To perform a sensitivity analysis for finding out the most sensitive variable with respect to breakthrough time, for each variable a certain deviation (positive and negative) with respect to the reference value was considered. The reference values selected for each variable and their deviations were listed in Table 3.

4.2.1. Effect of influent concentration on the breakthrough behavior

The effect of influent phenolic compounds concentration (C_0) on the form of the breakthrough curves was studied, while the other conditions were kept constant. The results for different influent phenolic compounds concentration in fixed-bed column of PPMS-based AC are shown in Fig. 4. At higher phenols inlet concentration, breakthrough curves were sharper leading to earlier breakthrough. With an increase of influent adsorbate concentration, the adsorbent active sites became more rapidly saturated and resulted in decrease of the breakthrough time. At low influent phenols concentration, breakthrough curves were expanded and breakthrough occurred gradually, indicating that a high volume of effluent solution could be processed. This was due to the fact that mass transfer coefficient become small when the inlet concentration decreased. With the increase of inlet concentration, concentration gradient between solution phase and solid phase increased. Therefore, adsorption rate increased and breakthrough curves were sharper but holding time in bed was smaller than the case of low-inlet concentration. This means adsorption capacity may not increase the same as mass transfer amount [41]. Similar results were reported in adsorption of phenol and other contaminants [42].

4.2.2. Effect of bed height on the breakthrough behavior

The bed height (H) is another effective parameter in the dynamic adsorption process in fixed-bed column due to the pressure drop and more important the weight of adsorbent loaded in column. To study this effect, the breakthrough curves of phenolic compounds adsorption were attained at 2, 4, and 6 cm the bed height, while the inlet concentration, inlet flow rate, and temperature were fixed. According to the obtained breakthrough curves (see Fig. 5), the breakthrough times were increased when the adsorbent bed height increased. This can be justified by knowing that with increasing adsorbent bed height (or the weight of adsorbent), the number of active sites on the adsorbent surface available in the column was increased. Thus, more phenolic compounds molecules could be adsorbed on the adsorbent surfaces and mass transfer zone is broadened. This means that more volume of effluent solution can be processed due to increase in the adsorption capacity. At the smaller fix-bed column height, saturation occurs faster due to limitation in the number of active binding sites onto the adsorbent surfaces as well as lack of sufficient time for adsorbate to diffuse into the internal pores of the adsorbent [42].

Table 4
Calculated parameters and determination coefficient (R^2) obtained for Yan, Thomas and ML-ANN models

			Column height (cm)			Temperature (°C)			Influent concentration (mg/l)			Inflow (ml/min)		
			2	4	6	20	35	50	60	100	140	2	3.5	5
Ph	Yan	K_Y	0.3682	0.4907	0.9464	0.3682	0.4979	0.3814	1.0667	0.4610	0.3682	0.1125	0.1609	0.3682
		q_Y	13.9864	19.7722	15.7170	13.9864	7.6377	8.0749	6.7758	13.9805	13.9864	118.3412	60.4163	13.9864
		R^2	0.9972	0.9969	0.9982	0.9972	0.9954	0.9934	0.9967	0.9959	0.9972	0.9985	0.9926	0.9972
	Thomas	K_{Th}	0.0035	0.0026	0.0032	0.0035	0.0067	0.0060	0.0079	0.0036	0.0035	0.0011	0.0012	0.0035
		q_{Th}	144.9587	272.2982	417.2742	144.9587	106.6823	86.5560	86.9300	129.8539	144.9587	150.8160	193.8303	144.9587
		R^2	0.9959	0.9957	0.9983	0.9959	0.9942	0.9955	0.9550	0.9936	0.9959	0.9967	0.9955	0.9959
	ANN	R^2	0.9982	0.9992	0.9993	0.9982	0.9986	0.9970	0.9999	0.9991	0.9982	0.9999	0.9995	0.9982
2-Cph	Yan	K_Y	0.2803	0.3366	0.7900	0.2803	0.2420	0.3019	0.6395	0.4280	0.2803	0.1527	0.2307	0.2803
		q_Y	21.3148	34.9257	21.6298	21.3148	17.7866	12.0241	15.1837	17.5955	21.3148	104.8854	50.9645	21.3148
		R^2	0.9969	0.9966	0.9939	0.9969	0.9952	0.9939	0.9932	0.9926	0.9969	0.9940	0.9983	0.9969
	Thomas	K_{Th}	0.0024	0.0014	0.0024	0.0024	0.0028	0.0041	0.0033	0.0028	0.0024	0.0012	0.0014	0.0024
		q_{Th}	169.0316	331.7085	479.0237	169.0316	122.2022	102.7187	117.8019	151.6614	169.0316	180.1422	232.0907	169.0316
		R^2	0.9968	0.9957	0.9933	0.9968	0.9908	0.9958	0.9954	0.9950	0.9968	0.9924	0.9969	0.9968
	ANN	R^2	0.9958	0.9974	0.9974	0.9958	0.9953	0.9966	0.9997	0.9993	0.9958	0.9985	0.9986	0.9958
4-Nph	Yan	K_Y	0.3556	0.2564	0.3096	0.3556	0.5079	0.3900	0.5588	0.2812	0.3556	0.1200	0.1875	0.3556
		q_Y	20.8025	60.7843	70.3553	20.8025	11.2286	13.4680	21.3468	32.2515	20.8025	155.7431	70.0840	20.8025
		R^2	0.9951	0.9969	0.9956	0.9951	0.9870	0.9951	0.9875	0.9949	0.9951	0.9960	0.9970	0.9951
	Thomas	K_{Th}	0.0024	0.0008	0.0007	0.0024	0.0052	0.0036	0.0023	0.0015	0.0024	0.0008	0.0010	0.0024
		q_{Th}	208.1303	442.2977	615.4835	208.1303	159.7194	147.9360	145.5469	185.7049	208.1303	211.7140	260.3146	208.1303
		R^2	0.9925	0.9937	0.9965	0.9925	0.9852	0.9942	0.9905	0.9915	0.9925	0.9946	0.9935	0.9925
	ANN	R^2	0.9993	0.9993	0.9993	0.9993	0.9947	0.9967	0.9996	0.9994	0.9993	0.9999	0.9988	0.9993

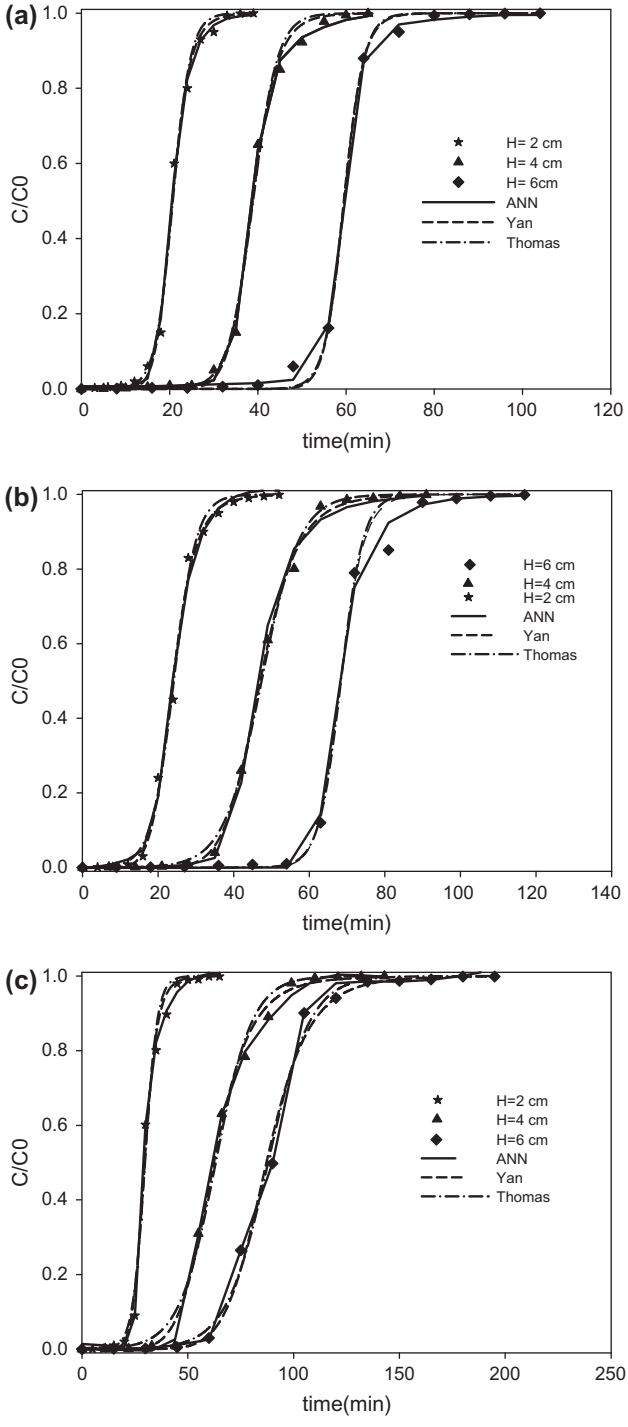

Fig. 5. Breakthrough curves containing experimental data and predicted values by ANN, Thomas and Yan models for adsorption of phenolic compounds onto the PPMS-based AC at different bed height [$C_0 = 140$ mg/l, $Q = 5$ ml/min and $T = 20$℃]. (a) ph, (b) 2-Cph, and (c) 4-Nph.

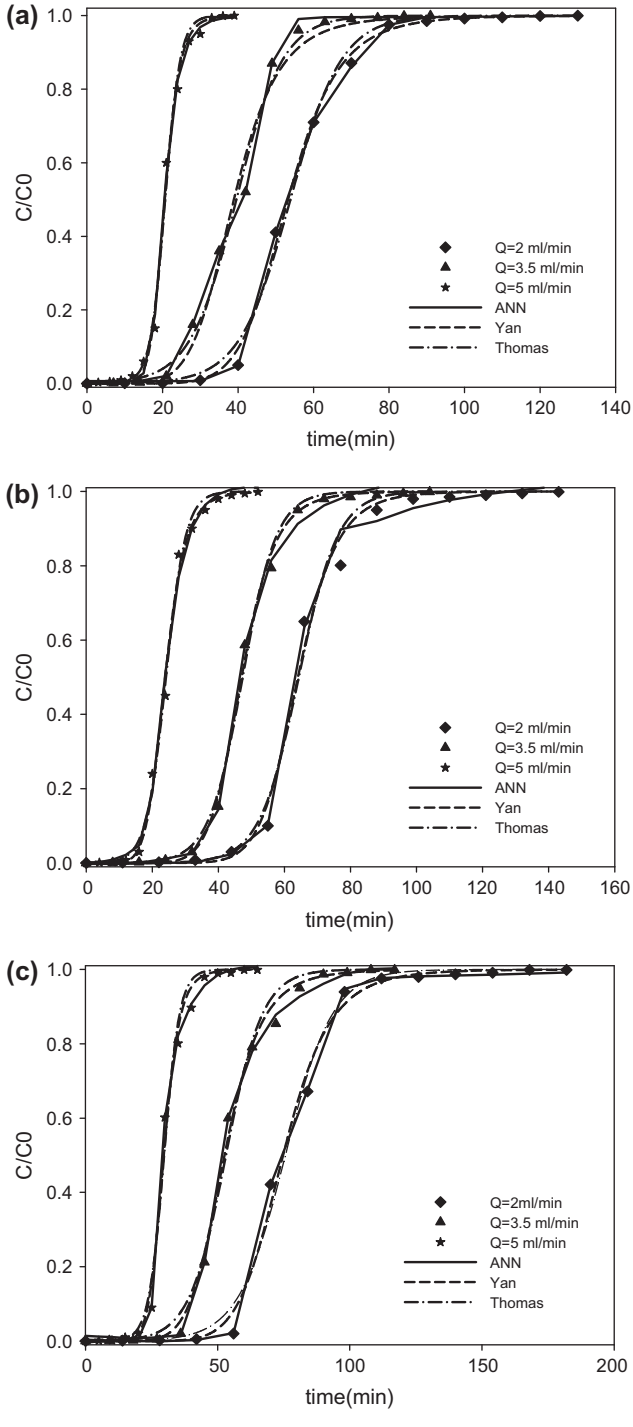

Fig. 6. Breakthrough curves including experimental data and predicted values by ANN, Thomas and Yan models for adsorption of phenolic compounds onto the PPMS-based AC at different flow rate [$H = 2$ cm, $C_0 = 140$ ml/min and $T = 20$℃]. (a) ph, (b) 2-Cph, and (c) 4-Nph.

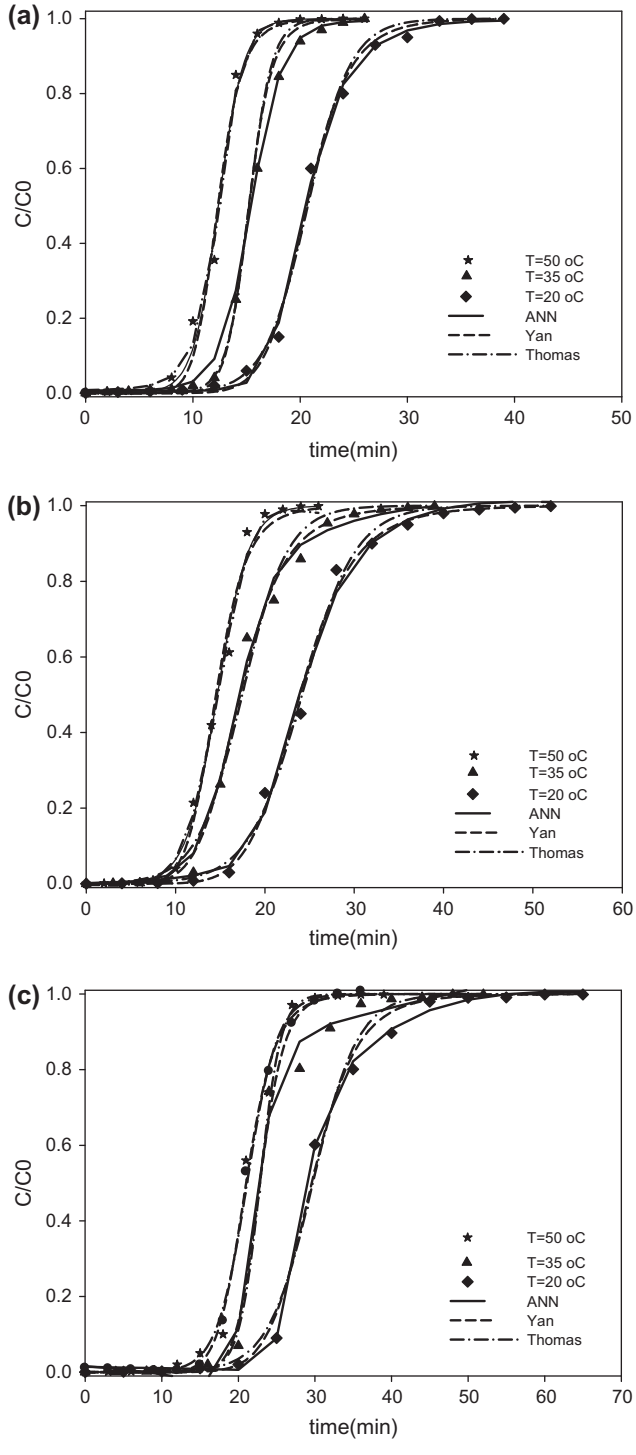

Fig. 7. Breakthrough curves including experimental data and predicted values by ANN, Thomas and Yan models for dynamic adsorption of phenolic compounds by PPMS-based AC at different temperature [$H = 2$ cm, $C_0 = 140$ ml/min and $Q = 2$ ml/min]. (a) ph, (b) 2-Cph, and (c) 4-Nph.

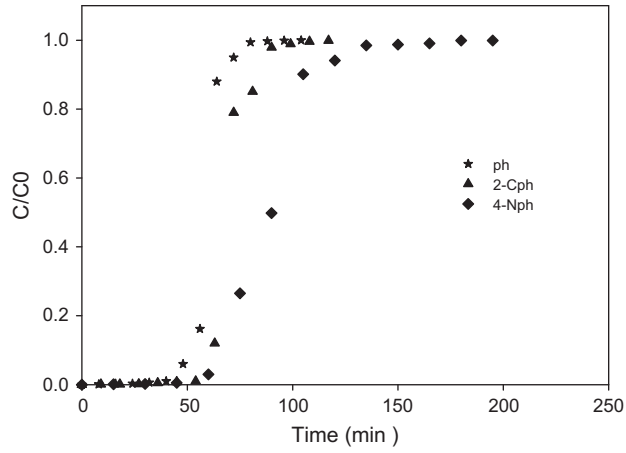

Fig. 8. Comparison of adsorption breakthrough curves for different phenolic compounds ($H = 6$ cm, $C_0 = 140$ ppm, $T = 20$ ℃ and $Q = 5$ ml/min).

4.2.3. Effect of feed flow rate on the breakthrough behavior

The effect of feed flow rate (Q) on the adsorption of phenolic compounds in the fixed-bed column packed with the PPMS-based AC was studied. The breakthrough curves of phenolic compounds adsorption were attained at 2, 3.5, and 5 ml/min flow rate while inlet concentration, bed height, and temperature were fixed. Fig. 6 shows the resulted experimental breakthrough curves. Residence time was shorter at higher feed flow rate causing inadequate diffusion of the phenolic compounds into the pores of the PPMS-based AC. Consequently, the phenolic compounds left the adsorption column before being adsorbed on the adsorbent bed. This led to reduction of the adsorption capacity of the phenolic compounds and hence, breakthrough time shifted towards earlier level.

4.2.4. Effect of temperature on the breakthrough behavior

The temperature (T) is one of the important parameters that effect on the adsorption capacity of adsorbent and also on the breakthrough curve. In order to investigate the effect of temperature on adsorption capacity of phenolic compounds by PPMS-based AC in fixed bed, the dynamic adsorption experiments were conducted at three various adsorption temperatures i.e. 20, 35, and 50 ℃. As illustrated in Fig. 7, the breakthrough times were demonstrated to decrease with the increase of temperature. This trend can be

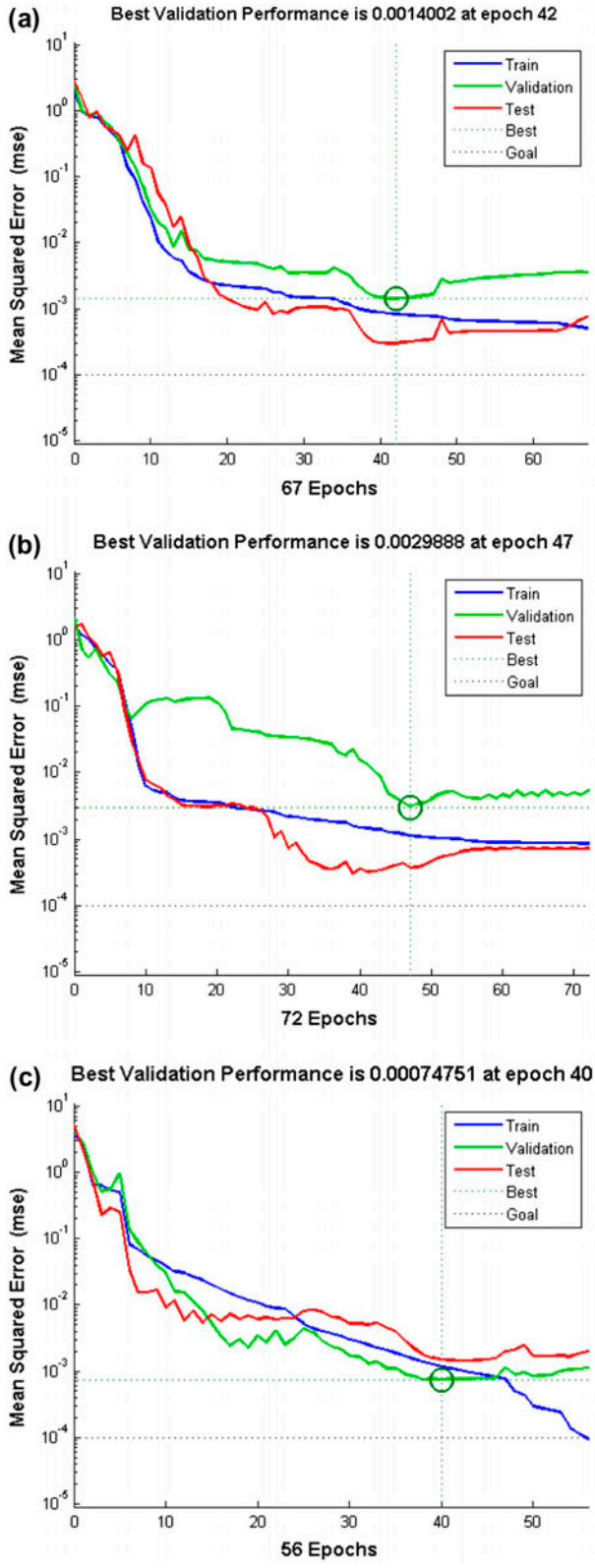

Fig. 9. Variation of MSE vs. epoch in training, validation and testing steps of ML-ANN for modeling of dynamic adsorption. (a) ph, (b) 2-Cph, and (c) 4-Nph.

attributed to the exothermic nature of adsorption process. Thus, the removal of phenolic compounds by PPMS-based AC developed in this study was more favorable at lower temperature i.e. 20˚C.

4.2.5. Comparative adsorption study of different phenolic compounds dynamic

To compare the breakthrough times of different phenolic compound used in the present study, the adsorption breakthrough curves obtained at fixed conditions for all adsorbates are shown in Fig. 8. As can be observed in Fig. 8, phenol breakthrough curve is the sharpest and 4-Nph breakthrough curve is the widest one, therefore, the breakthrough times followed the order of 4-Nph > 2-Cph > ph. The difference in the breakthrough time for different phenolic compounds can be attributed to their adsorption capacities which are highest for N-ph. The comparative adsorption capacities cannot be simply explained based on difference in molecular size. In fact, the adsorption capacity of an AC for uptake of phenolic compounds is mostly affected by the chemical nature of its surface, rather than its pore characteristics [43]. Substituent groups in the chemical structure of 4-Nph and 2-Cph, nitro and then chloro groups, act as a strong electron-withdrawing group which reduces the overall electron density in the π-bond of the aromatic ring. This implies that the attraction between the adsorbate and carbon surface is enhanced compared with interaction of phenol with the surface.

Besides, the most important functional group on the PPMS-based AC is hydroxyl group (as shown in FTIR spectrum) which plays a role in adsorption of all adsorbates. However, another functional group available on the AC surface based on FTIR spectrum is –N group in compounds such as quinine which may have an extra contribution to the higher adsorption of N-ph by the PPMS-based AC through reversible exchangeable reaction.

4.3. Modeling results

4.3.1. Physical models results

The values found for Thomas constants (K_{Th}) and Yan constants (q_Y and K_Y) for describing dynamic adsorption of different phenolic compounds at key operational conditions are summarized in Table 4 along with fitting determination coefficients (R^2). The results were further validated by Figs. 4–7(a–c) in which the predicted breakthrough curves and experimental points were shown at different inlet concentrations, bed depths, flow rates, and temperatures,

Table 5
Details of the designed ML-ANN to predict the dynamic adsorption of phenolic compounds in fixed-bed column

Details	Adsorbate		
	Ph	2-Cph	4-Nph
Input layer neurons	4	4	4
First hidden layer neurons	15	5	14
Second hidden layer neurons	2	8	12
Output layer neurons	1	1	1
Number of training data	106	106	106
Number of test data	20	20	20
Number of validation data	20	20	20
Transfer function in first hidden layer	Tansig	Tansig	Tansig
Transfer function in second hidden layer	Tansig	Tansig	Tansig
Transfer function in output layer	Purelin	Purelin	Purelin
Training algorithm	Trainlm	Trainlm	Trainlm
Learning algorithm	Learngdm	Learngdm	Learngdm
Epoch	67	72	56

Table 6
Contribution of input variables on the output variable (breakthrough time) (%)

Adsorbate	Bed height (H)	Liquid flow rate (Q)	Inlet concentration (C_i)	Temperature (T)
Ph	39.4	39.6	11.1	9.9
Cph	36.4	38.5	15.9	9.2
Nph	40.0	36.4	16.6	7.0

respectively. ANN model results were also shown for comparison in these figures.

4.3.2. ANN model results

To use ANN model, in this work, the number of layers and the number of neurons in each layer were analyzed with a learning rate of 0.01, training goal of 10^{-4}, and epochs 200 to obtain the best ML-ANN to be used to model dynamic adsorption of phenolic compounds from aqueous solution by PPMS-based AC. The number of neuron in the first and second hidden layers was tested in loop from 1 to 15 to give the minimum error. Regression coefficient selected as performance standard. When the regression coefficient of all data (testing and training and validation data) was higher than 0.999, training of ANN was stopped and the results were shown. This program was performed with Matlab software 7.14.0.739 (R2012.a). The performance of the formulated ML-ANN model was measured by mean square error (MSE) which is separately shown for all phenolic compounds in Fig. 9. As demonstrated in Fig. 9, the decreasing trends of MSE vs. epochs for testing and validation data are similar. Therefore, the probability of over-fitting error did not exist at interpolation.

The entire data-set (training, testing and validation data-set) was simulated by ML-ANN, then a linear regression between ML-ANN outputs and the corresponding targets was performed to survey performance of designed ML-ANN. Details of the designed ANN to model the dynamic adsorption of phenolic compounds by PPMS-based AC fixed-bed column are given in Table 5.

The performance of formulated ML-ANN model was measured by determination coefficients (R^2) which were all close to unity indicating a perfect match between experimental data and the model outputs (see Table 3). It was found that network with one hidden layer of neurons and different neurons in hidden layer for each adsorbate was successfully acted to predict the dynamic adsorption of phenolic compounds onto the PPMS-based AC. Although both physical models (Yan and Thomas) showed to be able to describe the experimental data, the simulated ML-ANN model was best model for describing the dynamic adsorption of phenolic compounds in PPMS-based AC fixed-bed column. A sensitivity analysis

was carried out to evaluate the relative importance of different input variables on the ANN performance. For this purpose, the calculation was made based on the ANN output data to determine the contribution of each input variable on the ANN simulated output and the results are reported in Table 6.

The ANN simulated results show that the breakthrough time was mostly influenced by the liquid flow rate and bed height followed by the inlet concentration and temperature, respectively.

5. Conclusion

A new low-cost AC with high-textural properties was produced from sludge collected from wastewater treatment plant of the pulp and paper factory. The produced AC was exhibited to be a possible adsorbent for the removal of phenolic compounds from effluent solutions using fixed-bed adsorption column. The adsorption capacity the PPMS-based AC bed was strongly dependent on the operational conditions. A shorter breakthrough time was obtained at higher influent concentration, flow rate, and temperature, while the breakthrough time was longer at higher bed height. The breakthrough times for different phenolic compounds followed the order of 4-nitrophenol > 2-chlorophenol > phenol which was attributed to the difference in adsorption capacity of the adsorbates.

Further attempts were made theoretically to model the dynamic behavior of the fixed-bed column packed with PPMS-based AC as the adsorbent for the removal of phenolic compound from water. A data-oriented ANN was developed to predict the breakthrough times obtained at various operational conditions along with two well-established physical model i.e. Thomas and Yan models. The experimental data were fitted to Yan, Thomas, and ANN models using non-linear regression analysis. A comparison was made between experimental breakthrough curves and those predicted by all models based on calculated determination coefficient (R^2). The results indicated that although both empirical models were acted fairly good to predict the breakthrough curves but a nearly perfect match was obtained using data-oriented ANN model.

The results of the present study are promising from two views points. First, use of the prepared PPMS-based AC as an effective adsorbent could dual benefit of improving the adsorption economy as well as reducing environmental hazards due to limitation in disposing sludge. Second, it was shown that the data-oriented model such as ANN can serve as a powerful means for prediction of adsorption dynamic behavior.

References

[1] J. Figueiredo, N. Mahata, M. Pereira, M. Sánchez Montero, J. Montero, F. Salvador, Adsorption of phenol on supercritically activated carbon fibres: Effect of texture and surface chemistry, J. Colloid Interface Sci. 357 (2011) 210–214.
[2] A.C. Lua, Q. Jia, Adsorption of phenol by oil–palm-shell activated carbons in a fixed bed, Chem. Eng. J. 150 (2009) 455–461.
[3] Q.-S. Liu, T. Zheng, P. Wang, J.-P. Jiang, N. Li, Adsorption isotherm, kinetic and mechanism studies of some substituted phenols on activated carbon fibers, Chem. Eng. J. 157 (2010) 348–356.
[4] K. Rzeszutek, A. Chow, Extraction of phenols using polyurethane membrane, Talanta 46 (1998) 507–519.
[5] B. Özkaya, Adsorption and desorption of phenol on activated carbon and a comparison of isotherm models, J. Hazard. Mater. 129 (2006) 158–163.
[6] J.D. Rodgers, W. Jedral, N.J. Bunce, Electrochemical oxidation of chlorinated phenols, Environ. Sci. Technol. 33 (1999) 1453–1457.
[7] J. Bandara, J. Kiwi, C. Pulgarin, G. Pajonk, Catalytic oxidation and photo-oxidation of nitrophenols by strong oxidants generated *in situ* via CuO-aerogel, J. Mol. Catal. A: Chem. 111 (1996) 333–339.
[8] A. Annachhatre, S. Gheewala, Biodegradation of chlorinated phenolic compounds, Biotechnol. Adv. 14 (1996) 35–56.
[9] N. Serpone, E. Pelizzetti, Photocatalysis: Fundamentals and Applications, Wiley, New York, NY, 1989.
[10] E. Bayram, N. Hoda, E. Ayranci, Adsorption/electrosorption of catechol and resorcinol onto high area activated carbon cloth, J. Hazard. Mater. 168 (2009) 1459–1466.
[11] B. Hameed, A. Rahman, Removal of phenol from aqueous solutions by adsorption onto activated carbon prepared from biomass material, J. Hazard. Mater. 160 (2008) 576–581.
[12] S. Rengaraj, S.-H. Moon, R. Sivabalan, B. Arabindoo, V. Murugesan, Agricultural solid waste for the removal of organics: Adsorption of phenol from water and wastewater by palm seed coat activated carbon, Waste Manage. 22 (2002) 543–548.
[13] K. Mohanty, D. Das, M. Biswas, Preparation and characterization of activated carbons from *Sterculia alata* nutshell by chemical activation with zinc chloride to remove phenol from wastewater, Adsorption 12 (2006) 119–132.
[14] I. Tan, A. Ahmad, B. Hameed, Preparation of activated carbon from coconut husk: Optimization study on removal of 2,4,6-trichlorophenol using response surface methodology, J. Hazard. Mater. 153 (2008) 709–717.
[15] F.-C. Wu, R.-L. Tseng, Preparation of highly porous carbon from fir wood by KOH etching and CO_2 gasification for adsorption of dyes and phenols from water, J. Colloid Interface Sci. 294 (2006) 21–30.
[16] A. Namane, A. Mekarzia, K. Benrachedi, N. Belhaneche-Bensemra, A. Hellal, Determination of the adsorption capacity of activated carbon made from coffee grounds by chemical activation with ZnCl and H_3PO_4, J. Hazard. Mater. 119 (2005) 189–194.

[17] N. Tancredi, N. Medero, F. Möller, J. Píriz, C. Plada, T. Cordero, Phenol adsorption onto powdered and granular activated carbon, prepared from *Eucalyptus* wood, J. Colloid Interface Sci. 279 (2004) 357–363.
[18] A.-N.A. El-Hendawy, Influence of HNO_3 oxidation on the structure and adsorptive properties of corncob-based activated carbon, Carbon 41 (2003) 713–722.
[19] A. Aygün, S. Yenisoy-Karakaş, I. Duman, Production of granular activated carbon from fruit stones and nutshells and evaluation of their physical, chemical and adsorption properties, Micropor. Mesopor. Mater. 66 (2003) 189–195.
[20] M. Otero, F. Rozada, L. Calvo, A. Garcıa, A. Moran, Elimination of organic water pollutants using adsorbents obtained from sewage sludge, Dyes Pigm. 57 (2003) 55–65.
[21] F. Rozada, M. Otero, J. Parra, A. Morán, A. García, Producing adsorbents from sewage sludge and discarded tyres: Characterization and utilization for the removal of pollutants from water, Chem. Eng. J. 114 (2005) 161–169.
[22] N. Khalili, J. Vyas, W. Weangkaew, S. Westfall, S. Parulekar, R. Sherwood, Synthesis and characterization of activated carbon and bioactive adsorbent produced from paper mill sludge, Sep. Purif. Technol. 26 (2002) 295–304.
[23] K. Pirzadeh, A.A. Ghoreyshi, Phenol removal from aqueous phase by adsorption on activated carbon prepared from paper mill sludge, Desalin. Water Treat. (2013), doi: 10.1080/19443994.2013.821034.
[24] H.C. Thomas, Heterogeneous ion exchange in a flowing system, J. Am. Chem. Soc. 66 (1944) 1664–1666.
[25] Y. Yavuz, A.S. Koparal, Electrochemical oxidation of phenol in a parallel plate reactor using ruthenium mixed metal oxide electrode, J. Hazard. Mater. 136 (2006) 296–302.
[26] A.B. Pandit, P.R. Gogate, S. Mujumdar, Ultrasonic degradation of 2:4:6 trichlorophenol in presence of TiO2 catalyst, Ultrason. Sonochem. 8 (2001) 227–231.
[27] A.G. Agrios, K.A. Gray, E. Weitz, Photocatalytic transformation of 2,4,5-trichlorophenol on TiO_2 under sub-band-gap illumination, Langmuir 19 (2003) 1402–1409.
[28] G. Yan, T. Viraraghavan, M. Chen, A new model for heavy metal removal in a biosorption column, Adsorpt. Sci. Technol. 19 (2001) 25–43.
[29] K. Yetilmezsoy, S. Demirel, Artificial neural network (ANN) approach for modeling of Pb(II) adsorption from aqueous solution by Antep pistachio (Pistacia Vera L.) shells, J. Hazard. Mater. 153 (2008) 1288–1300.
[30] K.V. Kumar, K. Porkodi, R.A. Rondon, F. Rocha, Neural network modeling and simulation of the solid/liquid activated carbon adsorption process, Ind. Eng. Chem. Res. 47 (2008) 486–490.
[31] R. Aghav, S. Kumar, S. Mukherjee, Artificial neural network modeling in competitive adsorption of phenol and resorcinol from water environment using some carbonaceous adsorbents, J. Hazard. Mater. 188 (2011) 67–77.
[32] L. Cavas, Z. Karabay, H. Alyuruk, H. Doğan, G.K. Demir, Thomas and artificial neural network models for the fixed-bed adsorption of methylene blue by a beach waste *Posidonia oceanica* (L.) dead leaves, Chem. Eng. J. 171 (2011) 557–562.
[33] E. Oguz, M. Ersoy, Removal of Cu^{2+} from aqueous solution by adsorption in a fixed bed column and neural network modelling, Chem. Eng. J. 164 (2010) 56–62.
[34] M.A. Dabhade, M. Saidutta, D. Murthy, Modeling of phenol degradation in spouted bed contactor using artificial neural network (ANN), Chem. Prod. Process Model. 3 (2008) 1138.
[35] F. Zeinali, A. Ghoreyshi, G. Najafpour, Adsorption of dichloromethane from aqueous phase using granular activated carbon: Isotherm and breakthrough cure measurement, Middle-East J. Sci. Res. 5 (2010) 191–198.
[36] K.V. Kumar, K. Porkodi, Modelling the solid–liquid adsorption processes using artificial neural networks trained by pseudo second order kinetics, Chem. Eng. J. 148 (2009) 20–25.
[37] R.-Q. Fu, T.-W. Xu, Z.-X. Pan, Modelling of the adsorption of bovine serum albumin on porous polyethylene membrane by back-propagation artificial neural network, J. Membr. Sci. 251 (2005) 137–144.
[38] N.G. Turan, B. Mesci, O. Ozgonenel, Artificial neural network (ANN) approach for modeling Zn(II) adsorption from leachate using a new biosorbent, Chem. Eng. J. 173 (2011) 98–105.
[39] N.G. Turan, B. Mesci, O. Ozgonenel, The use of artificial neural networks (ANN) for modeling of adsorption of Cu(II) from industrial leachate by pumice, Chem. Eng. J. 171 (2011) 1091–1097.
[40] T.G. Glover, M.D. LeVan, Sensitivity analysis of adsorption behavior: Experimentation of pulse inputs and layered-bed optimization, ChEnS 63 (2008) 2086–2098.
[41] J. Goel, K. Kadirvelu, C. Rajagopal, V. Kumar Garg, Removal of lead(II) by adsorption using treated granular activated carbon: Batch and column studies, J. Hazard. Mater. 125 (2005) 211–220.
[42] V.C. Taty-Costodes, H. Fauduet, C. Porte, Y.-S. Ho, Removal of lead (II) ions from synthetic and real effluents using immobilized *Pinus sylvestris* sawdust: Adsorption on a fixed-bed column, J. Hazard. Mater. 123 (2005) 135–144.
[43] A. Dąbrowski, P. Podkościelny, Z. Hubicki, M. Barczak, Adsorption of phenolic compounds by activated carbon—A critical review, Chemosphere 58 (2005) 1049–1070.